THE JOURNAL OF PHYSICAL CHEMISTRY B

Article

pubs.acs.org/JPCB

Membrane Potential Bistability in Nonexcitable Cells as Described by Inward and Outward Voltage-Gated Ion Channels

Javier Cervera,*[,†] Antonio Alcaraz,[‡] and Salvador Mafe*[,†]

[†]Departament de Termodinàmica, Universitat de València, E-46100 Burjassot, Spain

[‡]Department of Physics, Laboratory of Molecular Biophysics, University Jaume I, E-12080 Castellón, Spain

ABSTRACT: The membrane potential of nonexcitable cells, defined as the electrical potential difference between the cell cytoplasm and the extracellular environment when the current is zero, is controlled by the individual electrical conductance of different ion channels. In particular, inward- and outward-rectifying voltage-gated channels are crucial for cell hyperpolarization/depolarization processes, being amenable to direct physical study. High (in absolute value) negative membrane potentials are characteristic of terminally differentiated cells, while low membrane potentials are found in relatively depolarized, more plastic cells (e.g., stem, embryonic, and cancer cells). We study theoretically the hyperpolarized and depolarized values of the membrane potential, as well as the possibility to obtain a bistability behavior, using simplified models for the ion channels that regulate this potential. The bistability regions, which are defined in the multidimensional state space determining the cell state, can be relevant for the understanding of the different model cell states and the transitions between them, which are triggered by changes in the external environment.

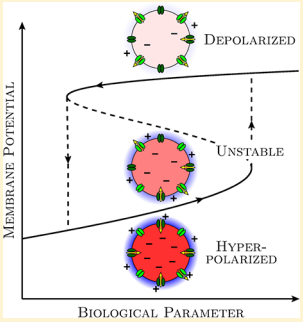

I. INTRODUCTION

The membrane potential is usually defined as the electrical potential difference between the cell cytoplasm and the extracellular environment when the current is zero. The coupling between this potential and the ionic gradients allows regulating the cell cycle and is relevant for cancer progress.[1−12] The ion channels in the cell membrane are essential for this regulation[3−5] because of the different electrical conductances shown by these aqueous nanopores.[8,9] In particular, inward- and outward-rectifying voltage-gated channels regulate the cell hyperpolarization (high membrane potential in absolute value) and depolarization (low membrane potential in absolute value) processes by means of ionic conduction and other permeation-independent mechanisms, dictating thus the values of this potential.[4−6,10−13]

Bistability is a key characteristic of the excitable cells in neuronal networks[14] and plays also an important role in nonexcitable cells.[15] Hyperpolarized and depolarized membrane potentials are significant parameters for carcinogenesis.[3,10] Usually, highly negative values of this potential are characteristic of terminally differentiated cells, in contrast with the relatively depolarized values found in more plastic cells (e.g., stem, embryonic, and cancer cells); see Figure 1 of refs 8 and 10. It is therefore of interest to study the transition between the cell hyperpolarized and depolarized states, as well as the possibility to obtain a bistability behavior, using simplified models and realistic biological parameters[4] for the ion channels that regulate the membrane potential.

Figure 1 schematically shows the problem we wish to consider here. The depolarized and hyperpolarized cell membrane potentials act as two states of a memory basic unit.[3] This biological unit shows bistability in the sense that transitions between the two potential states (see the dashed arrows in Figure 1) can be realized by appropriate changes in the relevant biological parameters. These changes may affect the internal characteristics of the cell membrane (e.g., the electrical properties of the ion channels) and the external conditions (e.g., the ionic concentrations and the pH value in the extracellular phase).

We attempt to develop a physical approach for the membrane potential bistability of a model nonexcitable cell using a minimum number of elements. This potential is regulated by a multiplicity of ion channels located on the cell membrane, but we consider only two basic channel characteristics (inward and outward electrical rectification[4]) which are physiologically relevant. We discuss the biological significance of the results obtained and provide clues useful for more detailed models incorporating additional cell elements.

We note also that nanoelectrodes, nanopores, and nanopipettes currently used for sensing and actuating can also benefit from the selective properties of the ion channels in biological membranes. In particular, the problem studied here may suggest simple physicochemical schemes to identify and exploit membrane potential bistability in practical applications. Single pores constitute the basic elements of multipore membranes and then bistability should be a useful property for processing signals, sensing, and actuating,[16] e.g., in analytical applications. To some extent, current nanofabrication techniques permit one to mimic biological properties using artificial single nanopores in functionalized membranes. Also, recon-

Received: August 17, 2014
Revised: October 6, 2014
Published: October 6, 2014

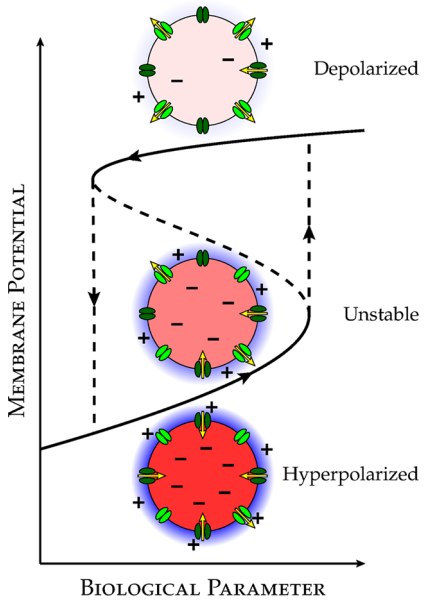

Figure 1. The depolarized cell (up state) corresponds to a low (in absolute value) negative membrane potential (e.g., −20 mV and low charge separation), while the hyperpolarized cell (bottom state) corresponds to a high (in absolute value) negative membrane potential (e.g., −70 mV and high charge separation). The model cell behaves as a dynamic biological unit showing transitions between the two bistable potential states when changes in the relevant biological parameters are externally induced. The inset cartoons schematically show the different cell electrical states and the inward- and outward-rectifying ion channels regulating the membrane potential.

stitution of ion channels on lipid bilayers allows a better control of the relevant biophysical parameters compared with the case of the cell membrane. Therefore, bistability phenomena could also be exploited in the ionic circuits characteristics of micro- and nanofluidics.[17]

II. BIOPHYSICAL CHARACTERISTICS OF VOLTAGE-GATED ION CHANNELS

The phenomenological characteristics of (e.g., potassium) inward-rectifying channels are shown in Figure 2a.[4−6,18−22] Relatively large inward currents can be conducted at potentials more negative than the equilibrium Nernst potential E_{in} (hyperpolarization), while low outward currents are obtained at potentials less negative than E_{in} (depolarization).[4] This phenomenological result is described by the following current (I)−potential (V) curve:

$$I = g(V - E_{in})P_{open}(V),$$
$$P_{open}(V) = \frac{1}{1 + \exp[zF(V - V_{th})/RT]} \quad (1)$$

where $P_{open}(V)$ is the channel open state probability, g is the maximum individual conductance, and V_{th} is a threshold potential.[4,18−22] The constants F, R, and T are, respectively, the Faraday constant, the gas constant, and the temperature. The parameter z describes the steepness between the open and closed conductance states and is usually interpreted as the effective number of channel charges involved in gating.[4]

We introduce now the following dimensionless variables in eq 1: $\tilde{I} = I/(gV_T)$, $\tilde{V} = V/V_T$, $\tilde{V}_{th} = V_{th}/V_T$, and $\tilde{E}_{in} = E_{in}/V_T$, where $V_T = RT/F = 27$ mV for $T = 310$ K. Then, eq 1 gives

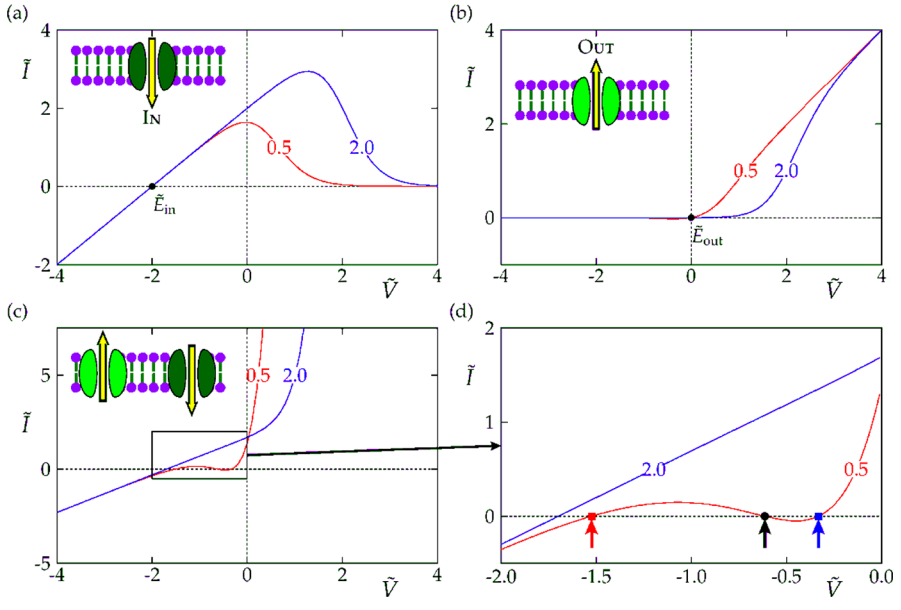

Figure 2. (a) $\tilde{I}$−$\tilde{V}$ curve of the inward-rectifying channel obtained from eq 2 for the equilibrium potential $\tilde{E}_{in} = E_{in}/V_T = -2$ (equivalent to $E_{in} = -54$ mV) and the gating charge $z = 3$.[4,19] The two threshold potentials $\tilde{V}_{th} = V_{th}/V_T = 0.5$ and 2.0 shown in the curves are equivalent to $V_{th} = 13.5$ and 54 mV. The above parameters are typical of voltage-gated channels.[4,13,15−19] (b) $\tilde{I}$−$\tilde{V}$ curve of the outward-rectifying channel obtained from eq 2 for the particular case of an equilibrium potential $\tilde{E}_{out} = E_{out}/V_T = 0$ and a gating effective charge $z = -3$. (c) The total current $\tilde{I}$, obtained from the individual currents $\tilde{I}_{in}$ and $\tilde{I}_{out}$, as a function of the potential $\tilde{V}$ for a system formed by $N_{in} = 1$ inward-rectifying channels with a maximum individual conductance g_{in} and an equilibrium potential $\tilde{E}_{in} = -1.7$ together with $N_{out} = 1$ outward-rectifying channels with a maximum individual conductance g_{out} and a potential $\tilde{E}_{out} = 0$. The total conductance ratio is defined as $G_{out}/G_{in} = N_{out}g_{out}/N_{in}g_{in} = 50$. (d) Inset of the bistability region in part c. The arrows show the three mathematical solutions obtained for the membrane potential $\tilde{V}_m = \tilde{V}(\tilde{I} = 0)$ in the case $\tilde{V}_{th} = 0.5$. The external points are the stable (red, hyperpolarized; blue, depolarized) values, while the central (black) point is the unstable value. The inset cartoons in parts a−c schematically show the ion channels inserted in the lipid bilayer of the cell membrane.

dx.doi.org/10.1021/jp508304h | J. Phys. Chem. B 2014, 118, 12444−12450

$$\tilde{I} = (\tilde{V} - \tilde{E}_{in})P_{open}(\tilde{V}),$$
$$P_{open}(\tilde{V}) = \frac{1}{1 + \exp[z(\tilde{V} - \tilde{V}_{th})]} \quad (2)$$

Figure 2a shows the $\tilde{I}-\tilde{V}$ curve obtained with eq 2. Note that $\tilde{V} = 2$ is equivalent to $V = 54$ mV and $\tilde{I} = 2$ is equivalent to $I = 54$ pA for a typical channel conductance $g = 1$ nS.[20−27] The $\tilde{I}-\tilde{V}$ curve of Figure 2b for an outward-rectifying channel can be obtained from eq 2 if we change the sign of z and substitute E_{out} for E_{in}.[4]

If $\tilde{E}_{in}$ is the equilibrium Nernst potential for potassium, then the membrane potential $\tilde{V}_m$ would be equal to $\tilde{E}_{in}$ in eq 2 only if we ignore the contributions of the sodium and chloride channels to this potential.[4,10] Figure 2a shows that the channel conductance takes high values for hyperpolarization ($\tilde{V} < \tilde{E}_{in}$) while it decreases for depolarization ($\tilde{V} > \tilde{E}_{in}$). This electrical rectification permits the cell membrane potential to be regulated because it constitutes a barrier to external stimuli.[21,22] Usually, the cell potential is not more negative than $\tilde{E}_{in}$ because the small outward current obtained for potentials more positive than $\tilde{E}_{in}$ keeps $\tilde{V}$ close to $\tilde{E}_{in}$ against the external depolarizing stimuli.[4] However, for $\tilde{V}$ higher than the critical potential corresponding to the maximum in the $\tilde{I}-\tilde{V}$ curves of Figure 2a, the channel closes and the differential conductance $d\tilde{I}/d\tilde{V}$ is negative. This closure can be due to external blockers and other internal gating processes[4,14,21−25] and depolarizes the potential $\tilde{V}$ to less negative values in Figure 2a. The channel enters then a region of potentials where it is no longer possible to maintain fixed the membrane potential against the external stimuli.[4,18,21] Remarkably, Figure 2a captures the observed experimental trends in most channels.[4,13−15,18−27] Note that the effect of the relevant ion (e.g., potassium) concentration and pH can be incorporated in the equilibrium potential $\tilde{E}_{in}$, while the channel characteristics are fully taken into account by the conductance g, the gating charge z, and the threshold potential $\tilde{V}_{th}$.[4,18,19]

The electrical characteristics can show a high diversity at the single channel level, and even for channels of the same type, individually different responses are usually observed.[26] This diversity of the responses results from the heterogeneities in the geometry and charge distributions of the individual channels. As an example, parts a and b of Figure 2 show the effect of different threshold potentials $\tilde{V}_{th}$ on the electrical responses of inward- and outward-rectifying channels, respectively.

The cell membrane is characterized by a multiplicity of electrically coupled channels.[30−34] However, the two generic voltage-gated ion channels of Figure 2a and b are crucial to determine the electrical cell characteristics and constitute then a simple minimum model to describe relevant basic functions. We consider now a cell with N_{in} inward-rectifying channels of individual conductance g_{in} and common potential $\tilde{E}_{in}$ in parallel with N_{out} outward-rectifying channels of individual g_{out} and common potential $\tilde{E}_{out}$. Figure 2c shows the total current corresponding to the inward- and outward-rectifying channels for the threshold potentials $\tilde{V}_{th,in} = \tilde{V}_{th,out} = \tilde{V}_{th}$ shown in the curves. Note the existence of a region with negative differential conductance (inset).

The membrane potential $\tilde{V}_m = \tilde{V}(\tilde{I} = 0)$ can now be obtained from the zero current condition, $N_{in}\tilde{I}_{in} + N_{out}\tilde{I}_{out} = 0$, which gives the dimensionless equation

$$(\tilde{V}_m - \tilde{E}_{in})\frac{1}{1 + \exp[z(\tilde{V}_m - \tilde{V}_{th,in})]} + \frac{G_{out}}{G_{in}}(\tilde{V}_m - \tilde{E}_{out})\frac{1}{1 + \exp[-z(\tilde{V}_m - \tilde{V}_{th,out})]} = 0 \quad (3)$$

to be solved for $\tilde{V}_m$ as a function of the relevant physiological parameters (note that $G_{out}/G_{in} = N_{out}g_{out}/N_{in}g_{in}$). Because of the electrical coupling between the different channels, three mathematical solutions of the membrane potential $\tilde{V}_m$ are obtained for certain values of these parameters (Figure 2c and d) which are realistic for voltage-gated channels.[4,13,17,20,21] The central value of $\tilde{V}_m$ corresponds to an unstable potential, which is located between the two stable hyperpolarized and depolarized potentials.

N-shaped $I-V$ curves and membrane potential bistability have been theoretically predicted using different models[28,33,34] and experimentally observed in the case of low enough extracellular potassium concentrations[34] (note that the equilibrium potential $\tilde{E}_{in}$ depends on this concentration[4]). Bistability is reported for individual skeletal and mouse lumbrical muscle cells.[32,34] The hair cell membrane shows also resting membrane potentials that fluctuate between two values which are determined by the potential region giving the low conductance range.[35] Finally, membrane potential measurements under inward rectification conditions yield (at least) two stable values due to the interplay of the inwardly rectifying channel with other electrical elements, as reported in different small mammalian cells (ref 36 and references therein). It must be noted that, in all the above cases, the inward-rectifying potassium channels are found to participate directly in the observed bistability phenomena.[32,34,35] Indeed, although detailed models of coupled differential equations corresponding to channels and pumps have been proposed to characterize the cell state,[30−33]voltage-gated channels are central in most cases because of their prominent physiological role.[3,8,13,24]

III. RESULTS AND DISCUSSION

A. Membrane Potential Bistability. Figures 3 and 4 show the membrane potential $\tilde{V}_m$ as a function of the relevant biological parameters $\tilde{E}_{in}$, G_{out}/G_{in}, and $\tilde{V}_{th,in} = \tilde{V}_{th,out} = \tilde{V}_{th}$ for $z = 3$ and $\tilde{E}_{out} = 0$. Figures 3a and 4a correspond to 3D plots, while Figures 3b and 4b are 2D projections of these plots on the $\tilde{V}_m-\tilde{E}_{in}$ plane. In each case, the unstable branch and the transitions between the two stable hyperpolarized and depolarized values of $\tilde{V}_m$ are shown. These transitions occur for high channel conductance ratios G_{out}/G_{in} (Figure 3b) and low threshold potentials $\tilde{V}_{th}$ (Figure 4b) because of the increased electrical sensitivity (Figure 2a).

Inward-rectifying potassium channels regulate the membrane potential during cell proliferation.[37] It has been reported that some tumor cell lines have anomalous inward-rectifying potassium channels which show biophysical characteristics different than the usual ones (compare Figure 6B with Figure 6A in ref 38). This experimental fact has a significant impact on the membrane resting potential (Figure 6C of ref 38; note that our parameter $\tilde{E}_{in}$ depends on the logarithm of the potassium concentration shown in the axis of this figure). Indeed, the membrane potential is significantly depolarized in tumor cells compared with normal cells, which may facilitate unlimited growth. Remarkably, the anomalous characteristics of the inward-rectifying potassium channel shown in Figure 6B of ref 38 resemble those of the outward-rectifying channel of Figure

dx.doi.org/10.1021/jp508304h | J. Phys. Chem. B 2014, 118, 12444−12450

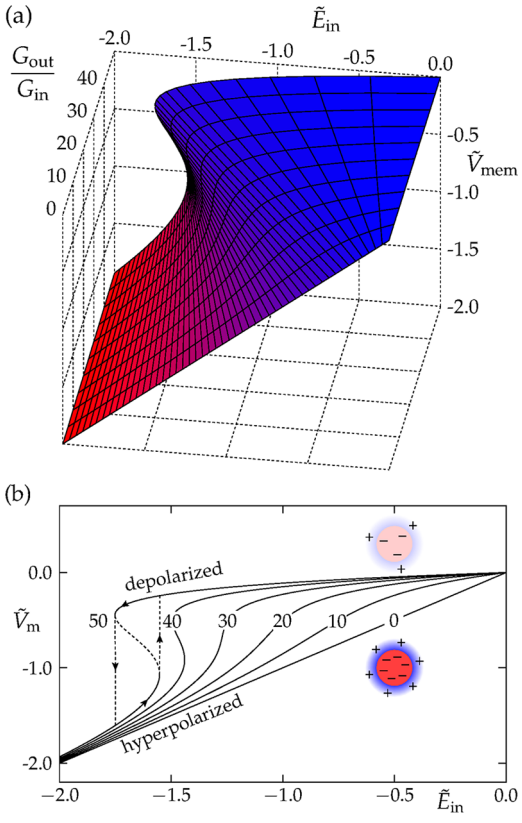

Figure 3. (a) 3D plot of the membrane potential $\tilde{V}_m$ as a function of $\tilde{E}_{in}$ and G_{out}/G_{in} for $z = 3$, $\tilde{V}_{th} = 0.5$, and $\tilde{E}_{out} = 0$. (b) The projection of part a on the $\tilde{V}_m$−$\tilde{E}_{in}$ plane is shown parametrically in G_{out}/G_{in}. Note the unstable branch (dashed line in the curve for $G_{out}/G_{in} = 50$) and the arrows showing the transitions between the two stable hyperpolarized and depolarized values of $\tilde{V}_m$ which are schematically shown in the cell cartoons.

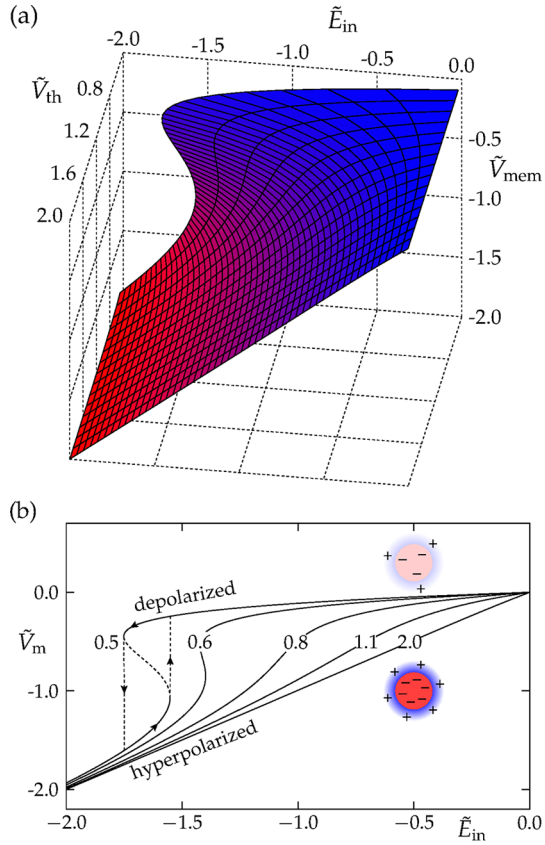

Figure 4. (a) 3D plot of the membrane potential $\tilde{V}_m$ as a function of $\tilde{E}_{in}$ and $\tilde{V}_{th}$ for $z = 3$, $G_{out}/G_{in} = 50$, and $\tilde{E}_{out} = 0$. (b) The projection of part a on the $\tilde{V}_m$−$\tilde{E}_{in}$ plane is shown parametrically in $\tilde{V}_{th}$. Note the unstable branch (dashed line for the curve $\tilde{V}_{th} = 0.5$) and the arrows showing the transitions between the two stable hyperpolarized and depolarized values of $\tilde{V}_m$ which are schematically shown in the cell cartoons.

2b here. Therefore, we could simulate the observed trends if we decrease the fraction of inward-rectifying channels (or, equivalently, increase the fraction of outward-rectifying channels) in our model, which is equivalent to increasing the channel conductance ratio G_{out}/G_{in} in eq 3. This fact forces the system to enter the bistability region where the depolarized state is also stable, suggesting that the results of Figure 3b may be of some relevance to the observed behavior.[38]

B. Phase Space. Figure 5 shows the multidimensional space characteristic of the membrane potential $\tilde{V}_m$. Note that the axes correspond to properties of the external solution (the equilibrium potential $\tilde{E}_{in}$ depends on the ionic concentrations and the pH value of the extracellular environment) and the channels (the ratio G_{out}/G_{in} is dictated by the number of channels and their individual conductances, while the threshold potential $\tilde{V}_{th}$ characterizes the electrical response). The experimental region where bistability occurs (the shaded surface in Figure 5) is only a limited subspace of the total space and can be obtained from the results of Figures 3 and 4. As an example, the insets show two points with the respective hyperpolarized and depolarized values of $\tilde{V}_m$ together with the unstable (black) value.

Levin[3] has recently suggested that cells characterized by common properties may cluster in different regions of a multidimensional state space where each axis defines a particular value of the relevant physiological parameter (e.g., an ionic concentration or a pH value). Figures 3b, 4b, and 5 tentatively show some realizations of the above suggestion. The cell state can flow between different states when appropriate changes are induced in the environment (Figure 2D of ref 3), which should be relevant for the external control of the cell cycle (e.g., by a pharmacological agent). Different physiological states and transitions between them can be described by changing the appropriate biological parameters in the axes (e.g., the threshold potential axis may be changed to a pH or calcium concentration axis and other dynamical equations for the new physiological variables can be added to the physical model). Note finally that the coordinate axes of Figure 5 include both electrochemical characteristics at the cellular level (the conductances and threshold potentials of the expressed ion channels) and biological conditions at the multicellular tissue level (the equilibrium potentials are regulated by the external ionic concentrations, and pH and can then vary with space and time according to these concentrations[4]).

C. Time Evolution. We have shown that the ideal biological unit considered here can exhibit membrane potential bistability for certain values of the internal characteristics and the external conditions (Figure 5). We address now the question of the time evolution of this potential, $\tilde{V}_m(\tilde{t})$, toward one of the two stable states. To this end, we introduce the simplifying assumption that the potential change is dictated solely by the instantaneous currents $\tilde{I}_{in}$ and $\tilde{I}_{out}$,[35,36] ignoring thus the slow changes in the ionic concentrations affecting the equilibrium potentials. These

dx.doi.org/10.1021/jp508304h | J. Phys. Chem. B 2014, 118, 12444−12450

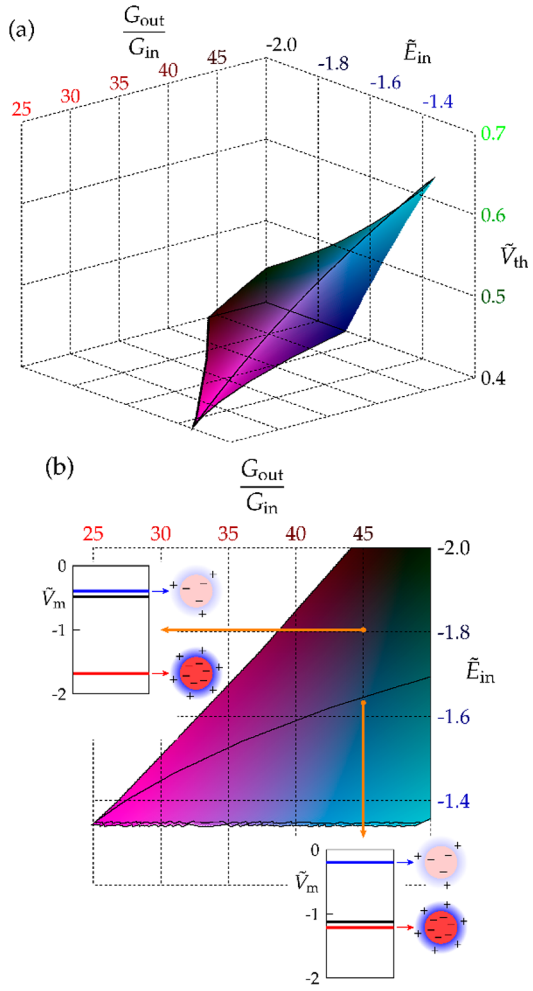

Figure 5. (a) The multidimensional state space of the membrane potential $\tilde{V}_m$ showing the limited experimental region (shaded surface) where bistability occurs can be obtained from the results of Figures 3 and 4. The region is truncated at the maximum ratio $G_{out}/G_{in} = 50$ and the minimum values $\tilde{E}_{in} = -2.0$ and $\tilde{V}_{th} = 0.4$ considered here. Note that each axis corresponds to a different biological parameter so that $\tilde{V}_m$ could flow between two given states, e.g., by changing the ionic concentrations that regulate the equilibrium potential $\tilde{E}_{in}$ or by decreasing the electrical channel conductance introducing an external blocker.[3] (b) The projection of part a on the G_{out}/G_{in}–$\tilde{E}_{in}$ plane. Two particular points have been marked on the bistability regions. The insets show the respective hyperpolarized (red) and depolarized (blue) stable values of $\tilde{V}_m$ together with the unstable (black) value.

changes, which may occur over long times,[32,34] should however be relevant in practical cases.

Figure 6 shows the change of the membrane potential as a function of time obtained from eqs 2 and 4:[35,36]

$$\frac{d\tilde{V}_m}{d\tilde{t}} = -(\tilde{I}_{in} + \tilde{I}_{out})/\tilde{C} \quad (4)$$

where $\tilde{C}$ and $\tilde{t}$ are the dimensionless electrical capacitance and time, respectively. Initially, the membrane potential $\tilde{V}_m(\tilde{t})$ is assumed to be close to the unstable branch of the curves in Figures 3b and 4b. When externally perturbed, the membrane potential $\tilde{V}_m(\tilde{t} = 0)$ will eventually reach one of the stable potentials.[33] The final (depolarized or hyperpolarized) potential will depend on the initial value: if $\tilde{V}_m(\tilde{t} = 0)$ is higher (in absolute value) than the unstable potential, $\tilde{V}_m(\tilde{t})$

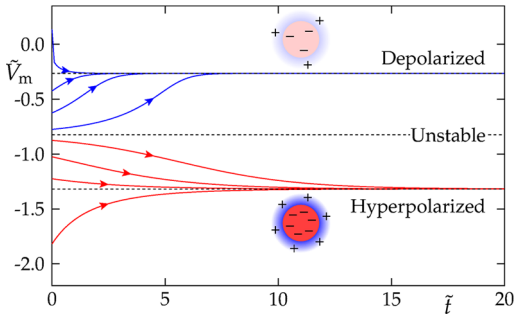

Figure 6. Membrane potential $\tilde{V}_m(\tilde{t})$ as a function of the dimensionless time $\tilde{t} = t/(C/G)$, where C and G are typical values for the electrical capacitance and conductance. For $C = 100$ pF and $G = 1$ nS,[36] the value $\tilde{t} = 10$ in the axis is equivalent to $t = 1$ s. The other biological parameters are $\tilde{V}_{th,in} = \tilde{V}_{th,out} = 0.5$ and $G_{out}/G_{in} = 50$. The curves are obtained from eqs 2 and 4 with $\tilde{E}_{in} = -1.6$ and $\tilde{E}_{out} = 0$. Upon external perturbation, the initial membrane potentials which are located in the vicinity of the unstable branch (Figures 3b and 4b) will evolve with time to either the depolarized or the hyperpolarized cell membrane potentials.

will relax toward the hyperpolarized cell state (Figure 6). On the contrary, if $\tilde{V}_m(\tilde{t} = 0)$ is lower (in absolute value) than the unstable potential, $\tilde{V}_m(\tilde{t})$ will relax toward the depolarized state. Examples of different time trajectories obtained from eq 4 are shown in Figure 6.

In summary, the results of Figures 3–6 give some insights into the multidimensional state space of a model cell membrane potential,[3] providing also some clues on the transition processes between the polarized and depolarized values. The physiological examples cited suggest that these results should be of qualitative value.[5,6,10,11,39,40] However, although the interplay between inward- and outward-rectifying voltage-gated channels has been shown here to be crucial for membrane potential regulation, the incorporation of other electrical elements (e.g., ion pumps and calcium channels[30−33]) is certainly necessary for the quantitative study of particular experimental cases.

IV. CONCLUSIONS

The nonexcitable cell cycle is characterized by changes in the membrane potential that are regulated by the conductance of different ion channels over the membrane. We have used a phenomenological model which constitutes a very simplified picture for the intricate mutual influence of ionic concentrations and potentials. The model makes use of the experimental fact that inward- and outward-rectifying voltage-gated channels dictate the potassium permeability of cells and are then involved in hyperpolarization and depolarization processes.[4,15] Therefore, these channels permit fundamental biological questions to be analyzed on a scale much more simple than the whole cell membrane, providing a necessary step to the subsequent incorporation of other elements which are needed for more complete descriptions.

The membrane potential is now experimentally identified as a key parameter in cell biology which is regulated by a multiplicity of ion channels and transporters, especially by voltage-gated channels.[3,5,10,11,39−41] Terminally differentiated cells tend to be highly polarized, showing a high (in absolute value) negative membrane potential. On the contrary, more plastic cells are relatively depolarized, showing a low (in absolute value) membrane potential. The membrane potential

dx.doi.org/10.1021/jp508304h | J. Phys. Chem. B 2014, 118, 12444−12450

bistability regions obtained here are within a multidimensional state space described by biological coordinates. Transitions between the different cell states could be triggered by changes in the external environment characteristics.[3] These characteristics are incorporated as the coordinate axes of Figures 3b, 4b, and 5 in each particular case, suggesting different mechanisms (trajectories in the state space) to modify the model cell state. In general, the coordinate axes should include electrochemical characteristics at the cellular level and biological conditions at the multicellular, tissue level (both properties are important for carcinogenesis[42]).

The membrane potential bistability may show some similarity to the *on*/*off* characteristic behavior of the basic element in a computer memory.[3] However, the biological counterpart follows a complex dynamics regulated by both internal and external properties because of the bioelectrochemical coupling between the channels in the cell membrane and between the individual cells in a tissue. We have addressed here only the first coupling for the simple but relevant case of inward- and outward-rectifying voltage-gated channels.

AUTHOR INFORMATION

Corresponding Authors

*Phone: +34 96 354 3926. E-mail: javier.cervera@uv.es.
*Phone: +34 96 354 3119. E-mail: smafe@uv.es.

Notes

The authors declare no competing financial interest.

ACKNOWLEDGMENTS

We acknowledge the financial support from the Generalitat Valenciana (project PROMETEO/GV/0069), the Ministry of Economic Affairs and Competitiveness (project MAT2012-32084 and project FIS2013-40473-P), and FEDER. We acknowledge Dr. Michael Levin, Biology Department and Tufts Center for Regenerative and Developmental Biology, Tufts University, for helpful comments on the manuscript.

REFERENCES

(1) McCaig, C. D.; Rajnicek, A. M.; Song, B.; Zhao, M. Controlling Cell Behavior Electrically: Current Views and Future Potential. *Physiol. Rev.* **2005**, *85*, 943−978.

(2) McCaig, C. D.; Song, B.; Rajnicek, A. M. Electrical Dimensions in Cell Science. *J. Cell Sci.* **2009**, *122*, 4267−4276.

(3) Levin, M. Molecular Bioelectricity in Developmental Biology: New Tools and Recent Discoveries. Control of Cell Behavior and Pattern Formation by Transmembrane Potential Gradients. *Bioessays* **2012**, *34*, 205−217.

(4) Hille, B. *Ion Channels of Excitable Membranes*; Sinauer Associates: Sunderland, MA, 1992.

(5) Urrego, D.; Tomczak, A. P.; Zahed, F.; Stühmer, W.; Pardo, L. A. Potassium Channels in Cell Cycle and Cell Proliferation. *Philos. Trans. R. Soc., B* **2014**, *369*, No. 20130094.

(6) Dahal, G. R.; Rawson, J.; Gassaway, B.; Kwok, B.; Tong, Y.; Ptácek, L. J.; Bates, E. An Inwardly Rectifying K^+ Channel is Required for Patterning. *Development* **2012**, *139*, 3653−3664.

(7) Shi, R.; Borgens, R. B. Three-Dimensional Gradients of Voltage During Development of the Nervous System as Invisible Coordinates for the Establishment of Embryonic Pattern. *Dev. Dyn.* **1995**, *202*, 101−114.

(8) Levin, M. Large-Scale Biophysics: Ion Flows and Regeneration. *Trends Cell Biol.* **2007**, *17*, 262−270.

(9) Adams, D. S.; Levin, M. Endogenous Voltage Gradients as Mediators of Cell-Cell Communication: Strategies for Investigating Bioelectrical Signals During Pattern Formation. *Cell Tissue Res.* **2013**, *352*, 95−122.

(10) Yang, M.; Brackenbury, W. J. Membrane Potential and Cancer Progression. *Front. Physiol.* **2013**, *4*, 185.

(11) Fiske, J. L.; Fomin, V. P.; Brown, M. L.; Duncan, R. L.; Sikes, R. A. Voltage-Sensitive Ion Channels and Cancer. *Cancer Metastasis Rev.* **2006**, *25*, 493−500.

(12) Perathoner, S.; Daane, J. M.; Henrion, U.; Seebohm, G.; Higdon, C. W.; Johnson, S. L.; Nüsslein-Volhard, C.; Harris, M. P. Bioelectric Signaling Regulates Size in Zebrafish Fins. *PLoS Genet.* **2014**, *10*, No. e1004080.

(13) Anumonwo, J. M. B.; Lopatin, A. N. Cardiac Strong Inward Rectifier Potassium Channels. *J. Mol. Cell. Cardiol.* **2010**, *48*, 45−54.

(14) Zhdanov, V. P. A Neuron Model Including Gene Expression: Bistability, Long-Term Memory, etc. *Neural Process Lett.* **2014**, *39*, 285−296.

(15) van Heukelom, J. S. The Role of the Potassium Inward Rectifier in Defining Cell Membrane Potentials in Low Potassium Media, Analyzed by Computer Simulation. *Biophys. Chem.* **1994**, *50*, 345−360.

(16) Ramirez, P.; Cervera, J.; Ali, M.; Ensinger, W.; Mafe, S. Logic Functions with Stimuli-Responsive Single Nanopores. *ChemElectroChem* **2014**, *1*, 698−705.

(17) Maglia, G.; Heron, A. J.; Hwang, W. L.; Holden, M. A.; Mikhailova, E.; Li, Q.; Cheley, S.; Bayley, H. Droplet Networks with Incorporated Protein Diodes Show Collective Properties. *Nat. Nanotechnol.* **2009**, *4*, 437−440.

(18) Lu, Z. Mechanism of Rectification in Inward-Rectifier K^+ Channels. *Annu. Rev. Physiol.* **2004**, *66*, 103−129.

(19) Cervera, J.; Mafe, S. Threshold Diversity Effects on the Electric Currents of Voltage-Gated Ion Channels. *EPL* **2013**, *102*, No. 68002.

(20) Newman, E. A. Inward-rectifying Potassium Channels in Retinal Glial (Müller) Cells. *J. Neurosci.* **1993**, *13*, 3333−3345.

(21) Oliver, D.; Baukrowitz, T.; Fakler, B. Polyamines as Gating Molecules of Inward-rectifier K1 Channels. *Eur. J. Biochem.* **2000B**, *267*, 5824−5829.

(22) Fakler, B.; Brändle, U.; Glowatzki, E.; Weidemann, S.; Zenner, H.-P.; Ruppersberg, J. P. Strong Voltage-Dependent Inward Rectification of Inward Rectifier K^+ Channels Is Caused by Intracellular Spermine. *Cell* **1995**, *80*, 149−154.

(23) Queralt-Martin, M.; Garcia-Gimenez, E.; Aguilella, V. M.; Ramirez, P.; Mafe, S.; Alcaraz, A. Electrical Pumping of Potassium Ions Against an External Concentration Gradient in a Biological Ion Channel. *Appl. Phys. Lett.* **2013**, *103*, No. 043707.

(24) von Beckerath, N.; Dittrich, M.; Klieber, H.-G.; Daut, J. Inwardly Rectifying K^+ Channels in Freshly Dissociated Coronary Endothelial Cells from Guinea-Pig Heart. *J. Physiol.* **1996**, *491*, 357−365.

(25) Panama, B. K.; Lopatin, A. N. Differential Polyamine Sensitivity in Inwardly Rectifying Kir2 Potassium Channels. *J. Physiol.* **2006**, *571*, 287−302.

(26) Arcangeli, A.; Bianchi, L.; Becchetti, A.; Faravelli, L.; Coronnello, M.; Mini, E.; Olivotto, M.; Wanke, E. A Novel Inward-rectifying K^+ Current with a Cell-cycle Dependence Governs the Resting Potential of Mammalian Neuroblastoma Cells. *J. Physiol.* **1995**, *489*, 455−471.

(27) Tang, W.; Yang, X.-C. Cloning a Novel Human Brain Inward Rectifier Potassium Channel and Its Functional Expression in Xenopus Oocytes. *FEBS Lett.* **1994**, *348*, 239−243.

(28) Léonetti, M.; Dubois-Violette, E.; Homblé, F. Pattern Formation of Stationary Transcellular Ionic Currents in Fucus. *Proc. Natl. Acad. Sci. U. S. A.* **2004**, *101*, 10243−10248.

(29) Kline, D.; Robinson, K. R.; Nuccitelli, R. Ion Currents and Membrane Domains in the Cleaving Xenopus Egg. *J. Cell Biol.* **1983**, *97*, 1753−1761.

(30) Fraser, J. A.; Huang, C. L.-H. Quantitative Techniques for Steady-state Calculation and Dynamic Integrated Modelling of Membrane Potential and Intracellular Ion Concentrations. *Prog. Biophys. Mol. Biol.* **2007**, *94*, 336−372.

(31) Jacquemet, V. Steady-state Solutions in Mathematical Models of Atrial Cell Electrophysiology and Their Stability. *Math. Biosci.* **2007**, *208*, 241−269.

(32) Gallahera, J.; Biera, M.; van Heukelom, J. S. First Order Phase Transition and Hysteresis in a Cell's Maintenance of the Membrane Potential -An Essential Role for the Inward Potassium Rectifiers. *Biosystems* **2010**, *101*, 149−155.
(33) Léonetti, M. On Biomembrane Electrodiffusive Models. *Eur. Phys. J. B* **1998**, *2*, 325−340.
(34) van Mila, H.; van Heukelom, J. S.; Bier, M. A Bistable Membrane Potential at Low Extracellular Potassium Concentration. *Biophys. Chem.* **2003**, *106*, 15−21.
(35) Jørgensen, F.; Kroese, A. B. A. Ion Channel Regulation of the Dynamical Instability of the Resting Membrane Potential in Saccular Hair Cells of the Green Frog (Rana Esculenta). *Acta Physiol. Scand.* **2005**, *185*, 271−290.
(36) Wilson, J. R.; Clark, R. B.; Banderali, U.; Giles, W. R. Measurement of the Membrane Potential in Small Cells Using Patch Clamp Methods. *Channels* **2011**, *5*, 530−537.
(37) Crociani, O.; Guasti, L.; Balzi, M.; Becchetti, A.; Wanke, E.; Olivotto, M.; Wymore, R. S.; Arcangeli, A. Cell Cycle-dependent Expression of HERG1 and HERG1B Isoforms in Tumor. *J. Biol. Chem.* **2003**, *278*, 2947−2955.
(38) Bianchi, L.; Wible, B.; Arcangeli, A.; Tagliatatela, M.; Morra, F.; Castaido, P.; Crociani, O.; Rosati, B.; Faravelli, L.; Olivotto, M.; et al. Encodes a K+ Current Highly Conserved in Tumors of Different Histogenesis: A Selective Advantage for Cancer Cells? *Cancer Res.* **1998**, *58*, 815−822.
(39) Lobikin, M.; Chernet, B.; Lobo, D.; Levin, M. Resting Potential, Oncogene-induced Tumorigenesis, and Metastasis: the Bioelectric Basis of Cancer *in vivo*. *Phys. Biol.* **2012**, *9*, No. 065002.
(40) Pardo, L. A.; Contreras-Jurado, C.; Zientkowska, M.; Alves, F.; Stühmer, W. Role of Voltage-gated Potassium Channels in Cancer. *J. Membr. Biol.* **2005**, *205*, 115−124.
(41) Funk, R. H. W.; Thiede, C. Ion Gradients and Electric Fields-An Intrinsic Part of Biological Processes. *J. Clin. Exp. Oncol.* **2014**, *S1*, 1−8.
(42) Sonnenschein, C.; Soto, A. M. Theories of Carcinogenesis: An Emerging Perspective. *Semin. Cancer Biol.* **2008**, *18*, 372−377.